

Transverse photon bunching and two-photon processes in the field of parametrically scattered light

D. N. Klyshko

Moscow State University

(Submitted 16 April 1982)

Zh. Eksp. Teor. Phys. **83**, 1313–1323 (October 1982)

The feasibility of observing paired spatial grouping of photon-detection points (e.g., on the screen of an image converter) is investigated. The effect can be used for absolute measurement of the quantum efficiency of an image converter. The correlation functions of the spontaneous parametric scattering field in the near zone and behind the collecting lens are calculated. The coherence scales of first and second order are determined. The coherence range in the near zone is bounded from below only by the width of the recorded angular spectrum in accordance with the uncertainty relation. It is demonstrated that the two-photon efficiency of the spontaneous parametric scattering field may exceed by several orders of magnitude the efficiency of the coherent field with the same intensity. This is readily explained by pair grouping of the photons. The influence of averaging over the detection volume, which suppresses the bunching effect, is assessed.

PACS numbers: 42.65.Jx, 42.80.Qy

INTRODUCTION

Spontaneous parametric scattering (SPS) is attributed to decay of photons passing through a transparent birefringent piezoelectric crystal, into a pair of photons that satisfy the synchronism conditions $\omega_0 = \omega + \tilde{\omega}$ and $\mathbf{k}_0 = \mathbf{k} + \tilde{\mathbf{k}}$. The photons in the pair are produced practically simultaneously, so that the secondary emission should consist of photons that are grouped in time into tight pairs.¹ We shall call this radiation for brevity two-photon light (TPL), and the pairs themselves will be called biphotons. The longitudinal distance between photons in a pair $l^{(2)}$ (the "length" of the biphoton) at the exit from the crystal is determined by the dispersion of the group velocity and usually does not exceed 1 mm (at a crystal length $l = 1$ cm). Such a longitudinal pair grouping of photons in SPS, confirmed by the coincidence method in Ref. 2, is used for absolute calibration of photodetectors.^{3,4} It is shown in the present paper that in SPS there should take place also a strong spatial or transverse grouping of the photons, due to the locality of the point of production of the biphoton. This effect should manifest itself in the near zone of the scattering region or in the zone of the real image of this region behind a converging lens (see Fig. 1). The locality of biphoton creation in time and in space follows from the phenomenological description of the SPS with the aid of the quadratic polarizability χ of the crystal (Ref. 3). In the transparency region one can neglect the frequency and spatial dispersion of χ and assume the energy density of the perturbation of the transverse macrofield inside the crystal to be $\chi E^3(\mathbf{r}, t)/3$, i.e., assume the interaction of the photons to be local. It follows therefore that the minimum transverse distance $\rho^{(2)}$ between the points of observation of photons belonging to one pair (the biphoton radius) is limited only by the Fourier uncertainty: $k_{\perp} \rho^{(2)} > 1$.

Thus, the image of the crystal (for example, on an image-converter screen) should consist partially of closely located or doubled points. The observation of the effect of paired transverse grouping would be a clear-cut proof of the

locality of the interaction, and by counting the relative number of double points it would be possible to determine the quantum efficiency of an image converter or of a vidicon.

The effect of photon grouping can be observed not only by the coincidence method (in time or in space), but also with the aid of stimulated multiphoton processes. It is known that grouping of photons in a random light (the Brown-Twiss effect) increases the probability of an m -photon process by a factor $m!$ compared with coherent emission with the same average intensity I . This gain g_m can be lucidly explained as being due to random superposition of wave packets that represent the photons, and a corresponding increase of the instantaneous intensity. In the TPL case, however, the grouping parameter $g \equiv g_2$ is much larger than two, this being due to "supergrouping"—regular congruence of the packets. The high two-photon efficiency of nondirectional TPL generated in spontaneous two-photon decay of excited states of atoms was noted in Ref. 5 and discussed in more detail in Ref. 6. For directed TPL emitted in SPS this question was considered in Ref. 7.

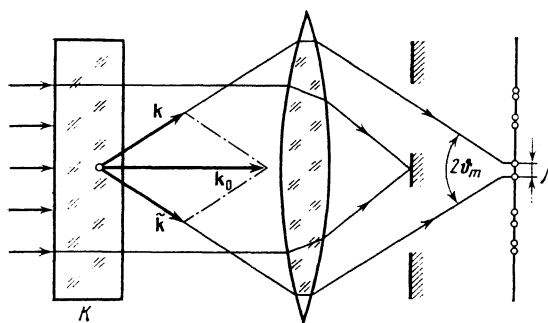


Fig. 1. Diagram of proposed experiment on the photography of biphotons. The image of the piezoelectric crystal K in parametrically scattered light can be produced by paired points with average distance $\langle \rho \rangle$ determined by the area radius $1/k\vartheta_m$ or by the crystal length $\vartheta_m l$.

It is typical that in the case of TPL the relative effect of the grouping g is proportional to $1/I$, i.e., to the average distance between the biphotons.^{1,7} A qualitative estimate of g can be obtained in the following manner. For a stimulated two-photon transition there must be present two photons in the coherence volume V_c , i.e., in the minimum volume of photon localization admissible by the uncertainty principle. In the case of coherent light, the probability P_2 of such a random paired grouping is determined by the Poisson distribution: $P_2 \approx \langle n \rangle^2 / 2!$, where $\langle n \rangle \ll 1$ is the average number of photons in V_c (i.e., the spectral brightness of the light in units of $\hbar c / \lambda^3$). In the case of TPL, however, the probability P_2' of observing the pair is equal to the average number of biphotons $\langle n' \rangle$ in V_c . At equal I we have $\langle n \rangle = 2 \langle n' \rangle$, so that the TPL is $g \equiv P_2' / P_2 = 1 / \langle n \rangle$ times more effective than coherent light.

To describe the absolute two-photon effectiveness of the radiation at a given point \mathbf{r} it is convenient to introduce a special photometric parameter, namely the two-photon intensity $I^{(2)} \equiv \sqrt{g} I$. Experimentally, g and $I^{(2)}$ can be determined from the decrease in the readings of a point wide-band two-photon detector on going from the measured radiation to coherent light having the same usual intensity $I^{(1)} \equiv I$. It will be shown below that in the SPS field $I^{(2)}$ is not only much stronger than I , but also has a higher directivity—the biphoton beam $I^{(2)}(\mathbf{r})$ is close in shape to the exciting pump beam $I_0(\mathbf{r})$ and has only approximately double the divergence, whereas $I(\mathbf{r})$ fills cone $2 \vartheta_m \sim 10^\circ$ (see Fig. 1).

We consider in this paper the following questions: the correlation functions of the SPS field in the near (Sec. 2) and far (Sec. 4) zones, as well as behind a converging lens (Sec. 5), the coherence scales of the first and second order (Sec. 3) and the influences exerted on them by the detection volume (Sec. 6), the photon distribution law in the transverse plane, and absolute measurement of the efficiency of an image converter or of a photographic film (Sec. 7).

1. CORRELATION FUNCTION OF SPS FIELD

The parameters introduced above are expressed in terms of the Glauber correlation functions (CF)⁸:

$$G_{1\dots m}^{(m)} \equiv \langle E_1^{(-)} \dots E_m^{(-)} E_1^{(+)} \dots E_m^{(+)} \rangle \equiv g_{1\dots m}^{(m)} G_1 \dots G_m, \quad (1)$$

$$I_1^{(m)} \equiv \frac{c}{2\pi\hbar\omega_1} G_{1\dots 1}^{(m)1/m}, \quad I^{(1)} \equiv I, \quad G^{(1)} \equiv G, \quad g_{12}^{(2)} \equiv g_{12}. \quad (2)$$

Here E_m is the field intensity at the point $\mathbf{x}_m \equiv \{\mathbf{r}_m, t_m\}$, $\omega_1 = ck_1$ is the central frequency, and $I_1^{(m)}$ is the m -photon intensity in x_1 (in photons/cm² sec). The connection between the first-order CF and $\langle n \rangle$ is of the form

$$G = (2\pi)^{-2} \hbar k_1^3 \Delta\omega_{\text{eff}} \Delta\Omega_{\text{eff}} \langle n \rangle = (\Delta\nu_{\text{eff}} \Delta\Omega_{\text{eff}} / 100, 1) \langle n \rangle, \quad (3)$$

where $\Delta\omega_{\text{eff}} = 2\pi c \Delta\nu_{\text{eff}}$ and $\Delta\Omega_{\text{eff}}$ are the effective frequency and angular widths of the spectra. The last equality in (3) expresses the first-order CF in Gaussian units at $\lambda_1 = 0.5 \mu\text{m}$.

According to Ref. 3 the CF are determined in the \mathbf{k} -representation by the crystal scattering matrix \mathbf{u} :

$$\langle a_1 a_2 \rangle = u_{12}, \quad \langle a_1^+ a_2 \rangle = \sum_s \dot{u}_{13} u_{23}, \quad (4)$$

$$\langle a_1^+ a_2^+ a_3 a_4 \rangle = \langle a_1^+ a_3 \rangle \langle a_2^+ a_4 \rangle + \langle a_1^+ a_4 \rangle \langle a_2^+ a_3 \rangle + \langle a_1^+ a_2^+ \rangle \langle a_3 a_4 \rangle, \quad (5)$$

$$u_{12} = \frac{2\pi}{\hbar} c_1 c_2 \delta(\omega_1 - \omega_2) \int d^3 r \chi E_0^{(+)}(\mathbf{r}) e^{-i(\mathbf{k}_1 + \mathbf{k}_2) \cdot \mathbf{r}}, \quad (6)$$

$$c_n = (\hbar \omega_n)^{1/2} / 2\pi, \quad \tilde{\omega} = \omega_0 - \omega,$$

where a_n^+ and a_n are the creation and annihilation operators for the scattered-light photons with wave vector \mathbf{k}_n (the field polarization in SPS is fixed by the synchronism condition), the length of the quantization box is assumed equal to 2π , while $E_0(\mathbf{r})$ is the pump field and assumed to be coherent and monochromatic.

The scattered-field intensity is

$$E(\mathbf{r}, t) = \sum_{\mathbf{k}} D_{\mathbf{r}\mathbf{k}} E_{\mathbf{k}}^{(+)} e^{-i\omega_{\mathbf{k}} t} + \text{H.c.}, \quad E_{\mathbf{k}}^{(+)} = i c_{\mathbf{k}} a_{\mathbf{k}}, \quad (7)$$

where the Green's function D in the case of a free field is equal to e^{ikr} , with $k = \omega/c$ outside the crystal and $k = n(\omega)/c$ inside the crystal (we neglect the refraction and reflection from the crystal faces).

With the aid of (4)–(7) we obtain the following integral expressions for the CF of the first two orders:

$$G_{12} \equiv \langle E_1^{(-)} E_2^{(+)} \rangle = \sum_{\mathbf{k}} R_{\mathbf{r}_1 \mathbf{k}}^* R_{\mathbf{r}_2 \mathbf{k}} e^{i\tilde{\omega}_{\mathbf{k}} t_1}. \quad (8)$$

$$G_{12}^{(2)} = G_1 G_2 + |G_{12}|^2 + |F_{12}|^2 \approx |F_{12}|^2, \quad (9)$$

$$R_{\mathbf{r}\mathbf{k}} \equiv i \sum_{\mathbf{k}'} D_{\mathbf{r}\mathbf{k}'} c_{\mathbf{k}'} u_{\mathbf{k}'\mathbf{k}}, \quad (10)$$

$$F_{12} \equiv \langle E_1^{(+)} E_2^{(+)} \rangle = - \sum_{\mathbf{k}_1 \mathbf{k}_2} D_{\mathbf{r}_1 \mathbf{k}_1} D_{\mathbf{r}_2 \mathbf{k}_2} c_{\mathbf{k}_1} c_{\mathbf{k}_2} u_{\mathbf{k}_1 \mathbf{k}_2} e^{-i\omega_1 t_1 - i\omega_2 t_2}. \quad (11)$$

The three terms in (5) and (9) describe respectively the random (Poisson) grouping of the photons, the excess grouping of the wave fields with Gaussian statistics (the Brown-Twiss effect), and the strong paired "supergrouping" which is typical of the TPL (at the points where $I^{(2)} \gg I$). We note that the relation between these terms depends substantially on the statistics of the pump field (for example, when pumping with two-photon light, the third term would correspond to four-photon grouping). It is easy to verify that the following connection holds

$$G_{12} = \frac{c}{2\pi i \hbar} \int d^3 r_3 F_{13} \int dt_3 F_{32}, \quad (12)$$

the function F_{12} contains therefore complete information on the SPS field (just as u_{12}).

According to (9), the probability of observing a biphoton at the point $\{x_1, x_2\}$ at $g_{12} \gg 1$ is proportional to $|F_{12}|^2$, therefore the function F_{12} plays the role of the wave function of the biphoton. We represent (11) in a somewhat different form:

$$F_{12} = \hbar \int d^4 x D(x_1 - x) D(x_2 - x) \chi E_0^{(+)}(x), \quad (13)$$

where

$$D(x) \equiv (2\pi)^{-2} \Sigma \omega_{\mathbf{k}} \exp(i\mathbf{k}\mathbf{r} - i\omega_{\mathbf{k}} t).$$

Equation (13) can be interpreted as follows: at each point of the crystal x there is a local spontaneous source of a biphoton

field with amplitude $\hbar\chi E_0^{(+)}(x)$, which is transported by the Green's functions $D(x)$ to the observation points x_1 and x_2 .

2. NEAR ZONE OF SPS

Let the angular spectrum of the recorded radiation be bounded by the angle $\vartheta_m = q_m/k \ll 1$. In practice ϑ_m is set by means of a diaphragm in the focal plane of the lens (see Fig. 1) or is specified by the synchronism condition. We define the near zone by the inequality $\rho < a_0 - \vartheta_m(z+l)$, in which $\rho = \{x, y\}$, l is the crystal length, the z axis is directed along the pump beam with radius a_0 , and the plane $z=0$ coincides with the exit face of the crystal. Let $l \ll k_0 a_0^2$; it is then obviously possible to put $a_0 = \infty$, i.e., assume the pump wave to be plane. The scattering matrix connects in this case only waves that satisfy the conditions for energy conservation and transverse-momentum conservation: $\tilde{\mathbf{q}} = -\mathbf{q}$. We restrict the transverse spectrum with the aid of the apodizing factor $\exp(-q^2/2q_m^2) \equiv Q$ for F_{12} and Q^2 for G_{12} (this violates the unitarity of the field transformation, but the use of an abrupt spectrum boundary⁷ leads to less clear results).

We shall distinguish hereafter between ω_k and $\omega_l = \omega_0/2$ and between the refractive index $n = ck/\omega$ and unity only in the wave detuning

$$\Delta(\omega, q) \equiv (k^2(\omega) - q^2)^{1/2} + (k^2(\bar{\omega}) - q^2)^{1/2} - k_0.$$

Let the collinear synchronism $\Delta(\omega, 0) = 0$ be satisfied for two frequencies $\omega^{(+)} > \omega_1$ and $\omega^{(-)} = \bar{\omega}^{(+)}$; we can then use the expansion

$$\Delta(\omega, q) \equiv \pm \alpha(\omega - \omega^{(\pm)}) - q^2/k_1, \quad \alpha \equiv 1/u^{(+)} - 1/u^{(-)},$$

$$u \equiv d\omega/dk.$$

We assume satisfaction of the condition $\Delta\omega \gg 2\pi/\alpha z_m$, where $\Delta\omega$ is the total width of the spectrum and $z_m \equiv k/q_m^2$. We introduce also the following notation:

$$\Delta\Omega_m = \pi\vartheta_m^2, \quad \Delta\omega_l = 2\pi/\alpha l, \quad \Gamma = 2\pi k_l \chi |E_0|, \\ \rho = |\rho_2 - \rho_1|, \quad z = z_2 - z_1, \quad \bar{z} = (z_1 + z_2)/2, \quad t = t_2 - t_1 - z/c.$$

With the aid of the quasi-optical approximation ($q \ll k$) we obtain the following estimates for the diffraction integrals (8) and (11):

$$F_{12} = -F\varphi\left(\frac{\rho q_m}{\sqrt{2}}, \frac{2\bar{z}}{z_m} + \frac{2|t|}{\alpha z_m}\right) \\ \times \sum_{(\pm)} \exp[i(k_0 z_2 - \omega_0 t_2 + \omega^{(\pm)} t)] \theta(\pm t), \quad (14)$$

$$G_{12} = \frac{G}{2} \left(1 - \frac{i|t|}{\alpha l}\right) \sum_{(\pm)} \varphi\left(\frac{\rho q_m}{2}, \frac{z}{2z_m} \pm \frac{t}{\alpha z_m}\right) e^{-i\omega^{(\pm)} t}, \quad (15)$$

$$I = \frac{G}{\Gamma l} = \frac{\hbar k_1^2}{2\pi^2} \Gamma l \Delta\omega_l \Delta\Omega_m, \quad \varphi(x, y) = \frac{1}{1+iy} e^{-x^2/(1+iy)}. \quad (16)$$

Here $|t| \ll \alpha l, 2\Delta\omega_l$ is the width of the spectrum at a fixed scattering angle, Γ has the meaning of the gain in parametric interaction of plane waves, and $\theta(t)$ is the step function. Comparison of (15) with (3) at $\Delta\omega_{\text{eff}} = 2\Delta\omega_l$ and $\Delta\Omega_{\text{eff}} = \Delta\Omega_m$ yields the spectral brightness and intensity of the SPS field:

$$\langle n \rangle = \Gamma^2 l^2 \sim 1.3 \cdot 10^{-7}, \quad I = I_{\text{vac}} \langle n \rangle \sim 0.8 \cdot 10^{12} \text{ cm}^2 \text{ sec}^{-1},$$

$$I_{\text{vac}} \equiv \Delta\omega_{\text{eff}} \Delta\Omega_{\text{eff}} / 2\pi\lambda_1^2 = 2\pi\vartheta_m^2 / \alpha l \lambda_1^2 \sim 6 \cdot 10^{18} \text{ cm}^2 \text{ sec}^{-1} \quad (17)$$

(in the estimates here and below we put $\lambda_1 = 0.5 \mu\text{m}$, $l = 1 \text{ cm}$, $\chi = 10^{-8}$ CGS, $\hbar\omega_0 I_0 = c|E_0|^2/2\pi = 1 \text{ W/cm}^2$, $\alpha = 0, 1/c$, $\vartheta_m = 5^\circ$, $z_m = 10 \mu\text{m}$, and $\Delta\nu_l = \Delta\omega_l/2\pi c = 10 \text{ cm}^{-1}$. Here I_{vac} is the intensity at which one photon passes through the coherence area $\lambda_1^2/\Delta\Omega_{\text{eff}}$ within the coherence time $2\pi/\Delta\omega_{\text{eff}}$.)

Substituting (14) and (15) in (9) we obtain the second-order CF:

$$G_{12}^{(2)} = G^2 g_{12} \approx F^2 f_{12}, \quad (18)$$

$$g_{12} = 1 + (|G_{12}|^2 + |F_{12}|^2)/G^2 \approx f_{12}/\langle n \rangle, \quad (19)$$

$$f_{12} = \frac{\theta(\alpha l - |t|)}{1 + \xi^2} \exp\left(\frac{-\rho^2 q_m^2}{1 + \xi^2}\right), \quad \xi = \frac{2(\bar{z} + |t|/\alpha)}{z_m}. \quad (20)$$

Thus, the grouping parameter in the near zone is

$$g = g_{11} = 2 + \langle n \rangle^{-1} (1 + 4z_1^2/z_m^2)^{-1}. \quad (21)$$

The two-photon intensity in the immediate vicinity of the crystal ($z_1 \ll z_m$) does not depend on the distance z_1 (just as the usual intensity I):

$$I_{\text{max}}^{(2)} = [I(I + I_{\text{vac}})]^{1/2} \approx \frac{2k_1^3 \chi \Delta\Omega_m}{\alpha} \left(\frac{\hbar I_0}{\lambda_0}\right)^{1/2} \sim 2 \cdot 10^{18} \text{ cm}^2 \text{ sec}^{-1}, \quad (22a)$$

and at $z_1 \gg z_m$ it decreases like $1/z_1$ (inasmuch as in this case a substantial contribution to $U^{(2)}$ is made only by longitudinal waves with $q \sim 0$):

$$I^{(2)} \approx I_{\text{max}}^{(2)} z_m / 2z_1. \quad (22b)$$

According to (22a), noticeable grouping takes place at $I \ll I_{\text{vac}}$, i.e., at $\Gamma l \ll 1$. We estimate the probability $W^{(2)}$ of direct two-photon ionization of cesium in the SPS field. The cross section of this process is of the order of $10^{-47} \text{ cm}^4 \cdot \text{sec}$ (Ref. 9), so that $W^{(2)} = \sigma^{(2)} I^{(2)2} \sim 4 \times 10^{-17} \text{ sec}^{-1}$. According to (22a), $W^{(2)}$ depends linearly on I_0 up to $I_0 \sim 10^7 \text{ W/cm}^2$, when $I^{(2)} \sim I \sim I_{\text{vac}}$ and $W^{(2)} \sim 10^{-10} \text{ sec}^{-1}$.

We note that the second-order CF and $I^{(2)}$ do not depend on the crystal length l at $\langle n \rangle \ll 1$ (Ref. 8) (up to $l_{\text{min}} \sim 2\pi/\alpha\Delta\omega$). The reason is that a fixed delay t the probability of observing two photons is governed only by emission from a thin layer l_{min} with a suitable distance $t|\alpha$ from the exit face (at $t=0$ only the exit face works). This independence of l is lost in the case of inertial detection (see below), as well as in degenerate synchronism, when $\omega^{(+)} = \omega^{(-)}$ and $\Delta\omega = \beta(\omega - \omega_1)^2$, where $\beta \equiv d^2 k^2/d\omega^2$. In the latter case the formulas presented above for the intensities I and $I^{(2)}$ at $l \gg z_m$ remain in force (accurate to coefficients of order of unity), if αz_m is replaced by $\sqrt{\beta l}$.

3. COHERENCE SCALES

At $\langle n \rangle \ll 1$ the function f_{12} (see (20)) determines the "form" of the biphoton, i.e., the probability of observing a pair of photons at the points x_1 and x_2 . Let $z_1 = z_2$; then f_{12} depends only on the differences $|\rho_1 - \rho_2| \equiv \rho$ and $|t_1 - t_2| \equiv t$ and on the distance to the crystal z_1 :

$$f_{12} = f(\rho, t) = \frac{\theta(\tilde{l} - \tilde{t})}{1 + (\tilde{z}_1 + \tilde{t})^2} \exp \left[\frac{-\tilde{\rho}^2}{1 + (\tilde{z}_1 + \tilde{t})^2} \right], \quad (23)$$

$$\tilde{\rho} = \rho q_m, \quad \tilde{t} = \frac{2t}{\alpha z_m}, \quad \tilde{z}_1 = \frac{2z_1}{z_m}, \quad \tilde{l} = \frac{2l}{z_m}, \quad z_m = \frac{k}{q_m^2}.$$

We define the effective second-order coherence time at $\rho = 0$ in the following manner:

$$t_{eff}^{(2)} = \frac{2}{f(0,0)} \int_0^\infty dt f(0, t) = \alpha z_m (1 + \tilde{z}_1^2) [\arctg(\tilde{z}_1 + \tilde{l}) - \arctg \tilde{z}_1] \\ = \begin{cases} \pi \alpha z_m / 2, & z_1 \ll z_m \ll l, \\ 2 \alpha z_1, & z_m \ll z_1 \ll l, \\ 2 \alpha l, & l \ll z_m \text{ or } z_1 \gg z_m, l. \end{cases} \quad (24)$$

Thus the average longitudinal distance $l^{(2)}$ between the photons in the pair (the biphoton length) changes from the reciprocal width of the spectrum

$$l_{min}^{(2)} = (2\Delta\nu_m)^{-1} \approx \pi \alpha z_m / 2 \sim 1.5 \mu\text{m}$$

(which is registered by the detector when account is taken of the conditions $\Delta = 0$ and $\vartheta < \vartheta_m$) near the crystal, to the reciprocal synchronism with $l_{max}^{(2)} = 2\Delta\nu_1^{-1} = 2\alpha c l \sim 0.2$ cm at large distances (in this case $t^{(2)}$ is determined by the relative delay of the signal and idle photons with average frequencies $\omega^{(+)}$ and $\omega^{(-)}$ inside the crystal).

The area and the coherence radius of second order at a given delay t is defined in similar fashion:

$$A_{eff}^{(2)} = \pi \rho_{eff}^{(2)2} = f^{-1}(0, t) \int dx dy f(x^2 + y^2, t) \\ = (\pi/q_m^2) [1 + (\tilde{z}_1 + \tilde{t})^2]. \quad (25)$$

From this, at $t = 0$ and $z_1 \ll z_m$, we have $\rho_{min}^{(2)} = 1/q_m \sim 1 \mu\text{m}$, and at $z_1 \gg z_m$ we have $\rho_{max}^{(2)} = 2\vartheta_m z_1 \sim 0.2 z_1$. Thus, the transverse distance between the points of observation of the simultaneously emitted photons is equal to the reciprocal width $1/q_m$, of the angular spectrum at short distances, and is equal to the distance to which the photons move apart at large distances. At $t \neq 0$, the radius $\rho^{(2)}$ increases, so that the photons manage to move apart prior to leaving the crystal.

We note that the effective quantities introduced above differ insignificantly from the averages over the distribution (23). For example, $\langle t \rangle = (2 \ln \tilde{l} / \pi^2) t_{eff}^{(2)}$ (at $\rho = z_1 = 0$ and $\tilde{l} \gg 1$) and $\langle \rho \rangle = (\sqrt{\pi}/2) \rho_{eff}^{(2)}$ (at $t = 0$).

The first-order coherence scales are determined by the CF of the same order (15). It is easy to verify that in the near zone $t^{(1)}$ and $\rho^{(1)}$ do not depend on z_1 and are close in order of magnitude to $t^{(2)}$ and $\rho^{(2)}$ at $\tilde{z}_1 \ll 1$. Thus, at $z_1 \ll z_m$ the photons and biophotons are approximately of equal size.

4. FAR ZONE

The Green's function in the (ω, r) representation at $r_1 \gg k_1 a_0^2$ is equal to

$$D_{r_1, -r_0} = \frac{1}{4\pi^2} \int d^2 q e^{i\mathbf{k}(r_1 - r)} \approx \frac{1}{i\lambda r_1} e^{i(kr_1 - k_1 r)}. \quad (26)$$

Substitution of this expression in (8) and (11) enables us to

estimate the CF for the SPS far zone. We introduce the notation $\mathbf{k}_n = k(\omega)\hat{\mathbf{r}}_n$, $\bar{\mathbf{k}}_n = k(\bar{\omega})\hat{\mathbf{r}}_n$, $\hat{\mathbf{r}} = \mathbf{r}/r$.

It follows from (26) and (11) that in the $a_0 = \infty$ approximation the contribution of waves with frequency ω to the biphoton wave function F_{12} is proportional to the spatial Fourier transform of the pump $\tilde{E}_0(\mathbf{k}_1 + \bar{\mathbf{k}}_2)$, i.e., in the case of a plane pump wave it is proportional to $\delta^{(3)}(\mathbf{k}_1 + \bar{\mathbf{k}}_2 - \mathbf{k}_0)$. In this case the two-photon intensity

$$I^{(2)}(\mathbf{r}_1) \sim \int_0^\infty d\omega E_0(\mathbf{k}_1 + \bar{\mathbf{k}}_1) \\ \sim \int_0^\infty d\omega \delta^{(3)}\left(\frac{n(\omega)\omega + n(\bar{\omega})\bar{\omega}}{c} \hat{\mathbf{r}}_1 - \mathbf{k}_0\right) \quad (27)$$

has a sharp maximum in the longitudinal direction, i.e., it duplicates approximately the directivity of the pump, and contributions are made only by plane waves satisfying the collinear synchronism $|k + \bar{k} - k_0|l < 2\pi$.

It can be shown that in the case of a TEM₀₀ pump with radius a_0 it follows from (11) and (26) that

$$I^{(2)}(0, 0, z_1) = \frac{2k_1^3 \chi \Delta\Omega_1}{\alpha} \left(\frac{\hbar I_0}{\lambda_0}\right)^{1/2} = \frac{k_1^3 \chi a_0}{\alpha z_1^2} \left(\frac{P_0}{c}\right)^{1/2}, \quad (28)$$

where $\Delta\Omega_1 \equiv A_0/z_1^2$, $A_0 \equiv \pi a_0^2/2$, and $P_0 = \hbar\omega_0 I_0 A_0$ is the pump power. This expression differs from (22a) in that $\Delta\Omega_m$ is replaced by $\Delta\Omega_1$. At the far-zone boundary $z_1 = k_1 a_0^2$ and (28) goes over smoothly into (22b).

The usual intensity I in the far zone is determined from (8) and (26) at $x_1 = x_2$; in the cone $\vartheta < \vartheta_m$ it is smaller than (28) by a factor $1/al$ (just as at $z_1 \ll z_m$).

5. FOCUSING OF BIPHOTONS

The simplest method of increasing $I^{(2)}$ at the observation point r_1 is to use a spherical pump wave converging towards r_1 . It can be shown that in this case $I^{(2)}$ is $2z_1/b_0$ times larger than (28), where $b_0 = k_0 a_0^2$ is the confocal pump parameter. However, only the central part of the angular spectrum of the SPS is used in this case, whereas in the near zone at $z_1 \ll z_m$ the entire transverse spectrum up to q_m is summed.

We consider the image of the near zone of the SPS produced with the aid of a converging lens (see Fig. 1). To this end it is necessary to regard $D_{r\mathbf{k}}$ in (7), (10), and (11) as the Green's function of an ideal apodized lens:

$$D_{r\mathbf{k}} = -\frac{z'}{z} \exp\left\{ikr + \frac{i}{2}kz' \left[\left(\frac{k_x}{k} - \frac{x}{r}\right)^2 + \left(\frac{k_y}{k} - \frac{y}{r}\right)^2\right]\right\}, \\ 1/z' \equiv 1/f' - 1/z, \quad 1/f' \equiv 1/f - i/kR^2, \quad (29)$$

where f is the focal length and R is the effective radius of the lens. Let $a_0 \gg R$, so that we can assume the pump wave to be plane. After integration we obtain the two-photon intensity at a distance z_1 on the axis behind the lens:

$$I^{(2)} = \frac{2k_1^3 \chi \Delta\Omega_f}{\alpha} \left(\frac{\hbar I_0}{\lambda_0}\right)^{1/2}, \quad \Delta\Omega_f \equiv \frac{\pi}{k_1 z_0 z_1^2} \left| \frac{1}{z_1'} \left(\frac{1}{z_1'} - \frac{1}{z_0} \right) \right|^{-1}, \quad (30)$$

where z_0 is the distance from the crystal to the lens and $\Delta\Omega_f$

plays the role of the effective solid angle (cf. (22a) and (28)). For example, at the focus ($z_1 = f$) at $z_0 \ll k_1 R^2$ this angle is equal to the solid angle $\pi R^2/f^2$ of the lens. On the other hand, if $1/z_0 + 1/z_1 = 1/f$, then $\Delta\Omega_f = \pi R^2/z_1^2$. We did not take into account here the restriction of the angular spectrum, so that in the general case it is necessary to replace $\Delta\Omega_f$ in (30) by $\min\{\Delta\Omega_f, \Delta\Omega_m\}$.

The second-order coherence radius $\rho^{(2)}(z_1)$ at a distance z_1 behind the lens at $z_1 = f$ is determined by the maximum photon-separation angle $\rho^{(2)}(f) \sim 2f\vartheta_m$, and at $z_1 = z_0 = 2f$ it is determined by the uncertainty relation $\rho^{(2)}(2f) \sim 1/q_m$. The coherence length is similarly transformed.

6. AVERAGE CORRELATION FUNCTIONS

In the course of detection there takes place inevitably a certain averaging of the CF, and this decreases the observed grouping effect.

We consider first averaging of the first-order CF with respect to time. According to (9),

$$\begin{aligned} \bar{G}_{12}^{(2)} &= \frac{1}{T^2} \int_0^T dt_1 dt_2 G_{12}^{(2)} \\ &= G_1 G_2 + \frac{2}{T} \int_0^T dt \left(1 - \frac{t}{T}\right) (|G_{12}|^2 + |F_{12}|^2), \end{aligned} \quad (31)$$

where T is the time constant of the detector and $z_1 = z_2$. Let $T \gg t^{(1)}$ and $T \gg t^{(2)}$; the contribution of G_{12} can then be neglected, and (31) takes, with allowance for (18)–(20), the form

$$\bar{G}_{12}^{(2)} = G^2 \bar{g}(\rho), \quad \bar{g}(\rho) = 1 + \bar{f}(\rho)/T \langle n \rangle, \quad (32)$$

$$\bar{f}(\rho) = 2 \int_0^{\alpha l} \frac{dt}{1 + (\tilde{z}_1 + \tilde{t})^2} \exp\left[-\frac{\rho^2}{1 + (\tilde{z}_1 + \tilde{t})^2}\right]. \quad (33)$$

The grouping parameter now differs from (21):

$$\bar{g}(0) = 1 + t_{\text{eff}}^{(2)} T^{-1} \langle n \rangle^{-1} (1 + 4z_1^2/z_m^2)^{-1}. \quad (34)$$

Let $z_1 \ll z_m \ll l$; then $t_{\text{eff}}^{(2)} = t_{\text{min}}^{(2)}$ and it follows from (17) and (32) that (cf. (22))

$$\bar{I}^{(2)} = \frac{1}{2\pi\hbar k_1} [\bar{G}^{(2)}]^{1/2} = \left[I \left(I + \frac{t_{\text{min}}^{(2)}}{T} I_{\text{vac}} \right) \right]^{1/2}, \quad (35)$$

so that the condition of assured observation of the grouping takes the form

$$\langle n \rangle \ll t_{\text{min}}^{(2)}/T = \alpha\lambda_1/4\vartheta_m^2 T \sim 5 \cdot 10^{-15}/T,$$

which is equivalent at $T = 1$ to a brightness temperature < 800 K or to an exposure (in photons per unit area)

$$H = IT \ll I_{\text{vac}} t_{\text{min}}^{(2)} = \pi/2\lambda_1 l \sim 3 \cdot 10^5 \text{ cm}^{-2}. \quad (36)$$

The effective coherence area can be defined in analogy with (25):

$$\bar{A}_{\text{eff}}^{(2)} = \bar{f}^{-1}(0) \int dx dy \bar{f}(\rho) = \lambda_1 l [\arctg(\tilde{z}_1 + l) - \arctg \tilde{z}_1]^{-1}. \quad (37)$$

At $z_1 \ll z_m \ll l$ we obtain $\bar{A}_{\text{eff}}^{(2)} = 2\lambda_1 l/\pi$.

We consider now the distribution density $p(\rho)$ for transverse biphoton dimensions ρ in the case of inertial detection. Let $\bar{g}(\rho) \gg 1$; we can then neglect unity in (32) and $p(\rho)$ is

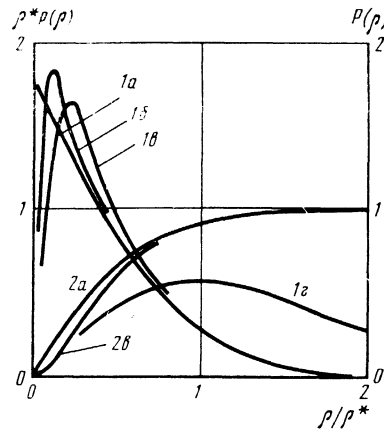


Fig. 2. Distribution density $p(\rho)$ (curve 1) and distribution function $P(\rho)$ (curves 2) of the probabilities of the distances ρ between the points of observation of photons in the case of inertial detection at various distances to the crystal z_1 and crystal lengths l (ρ is in units of $1/\rho^*$, and z_1 and l are in units of $1/k\vartheta_m^2$, $\rho^* = 2\vartheta_m l$): $a - z_1 = 0$, $l \gg 100$; $b - 0, 10$; $c - 0, 5$; $d - z_1 = l \gg 100$.

equal to (33) with an additional factor $\rho q_m^2/\alpha l$ (Fig. 2). In the case $z_1 \ll z_m \ll l$ the function $p(\rho)$ has a sharp maximum at $\rho \sim 1/q_m \sim 1 \mu\text{m}$ and a long "tail" in the region $\rho \sim 2\vartheta_m l \equiv \rho^* \sim 1 \text{ mm}$ (here p depends only on the ratio ρ/ρ^*). The average distance between the photons in the pairs is

$$\begin{aligned} \langle \rho \rangle &= \frac{\pi^{1/2}}{4\lambda_1 l q_m^3} \{t(1+t^2)^{1/2} + \ln[t + (1+t^2)^{1/2}]\}_{z_1}^{\tilde{z}_1+l} \\ &\approx \frac{\sqrt{\pi}}{2} \vartheta_m (l + 2z_1). \end{aligned} \quad (38)$$

The distribution function corresponding to $p(\rho)$ (Fig. 2) is

$$\begin{aligned} P(\rho) &= 1 - \frac{1}{l} \int_{z_1}^{\tilde{z}_1+l} dt \exp\left(-\frac{\rho^2 q_m^2}{1+t^2}\right) \\ &\approx 1 - \frac{\rho}{2\rho^*} \Gamma\left(-\frac{1}{2}, \frac{\rho^2}{\rho^{*2}}\right). \end{aligned} \quad (39)$$

It reaches a level 0.5 at $\rho \sim \langle \rho \rangle$. In (39), Γ is the incomplete gamma function.

The transverse-grouping effect will be clearly noticeable on an image converter screen if $\langle \rho \rangle$ is much less than the average distance between the flashes $(A/\langle N \rangle)^{1/2}$, where $\langle N \rangle \approx N^{(0)} + \eta AT I$ is the average number of flashes on the area A ; here $N^{(0)}$ is the number of background flashes, η is the quantum efficiency, and T is the observation time or the afterglow time (the longer of the two). From this we obtain a condition somewhat different from (36)

$$N^{(0)}/A \ll \eta I \langle \rho \rangle^{-2} = 4/\pi\vartheta_m^2 l^2 \sim 1.6 \cdot 10^2 \text{ cm}^{-2} \quad (40)$$

In the case of non-pointlike and inertial detection it is necessary to carry out additional averaging over the detector cross section A , which under the condition $A \gg \bar{A}^{(2)}$ lead to replacement of $\bar{f}(\rho)$ and $\bar{g}(\rho)$ in (32) by

$$\bar{f} = \frac{1}{A^2} \int d^2\rho_1 d^2\rho_2 \bar{f}(|\rho_1 - \rho_2|) = \frac{2\pi\alpha l}{A q_m^2}, \quad (41)$$

$$\bar{g} = 1 + \alpha l z_m \lambda_1 / T A \langle n \rangle = 1 + 1/IAT \quad (42)$$

Substituting (42) in (32), we obtain with allowance for (17)

$$\bar{I}^{(2)} = [I(I + 1/IAT)]^{1/2}. \quad (43)$$

Thus, in the case of "incoherent" detectors, for which $AT \gg \bar{A}^{(2)}$, the grouping effect appears only at $I < 1/IAT$, i.e., when there is not more than one photon in the detection

volume cTA (in place of the coherence volume in the case of coherent detectors).

7. DISTRIBUTION OF THE FLASHES ON THE SCREEN AND ABSOLUTE MEASUREMENTS OF IMAGE-CONVERTER EFFICIENCY

We subdivide the image of the scattering region on the image-converter screen into sections with area $A \gg A^{(2)}$ and let P_N be the probability of the appearance of N flashes on one section during a time $T \gg t^{(2)}$. Let the pump and the crystal be homogeneous over the cross section. The mean values over the sections and over the ensemble should then coincide, so that P_N is determined in terms of the CF.

According to Refs. 1 and 10, the generating function of P_N in the case of TPL is of the form

$$Q(x) = \exp(ax + bx^2/2).$$

In our case

$$a = N^{(0)} + \eta(N^{(1)} + 2N^{(2)}), \quad b = 2\eta^2 N^{(2)} = 2\eta^2 ATI, \quad (44)$$

where $N^{(0)}$ is the average number of dark flashes on the area A during the time T , $N^{(1)}$ is the average number of unpaired photons, and $N^{(2)}$ is the average number of biphotons. If $b \ll a$, then $Q(x)$ determines the Poisson distribution with $\langle N \rangle = a$. If, however, the number of background flashes $N^{(0)} + \eta N^{(1)}$ is small and $\eta = 1$, then $b = a$ and $Q(x)$ determines a Poisson distribution of the binary flashes:

$$P_{2N+1} = 0, \quad P_{2N} = [(a/2)^N / N!] e^{-a/2}.$$

In the general case it follows from $Q(x)$ that

$$\langle N \rangle = Q'(0) = a, \quad \langle N(N-1) \rangle = Q''(0) = a^2 + b, \quad (45a)$$

$$P_0 = Q(-1) = e^{-a+b/2}, \quad P_1 = Q'(-1) = (a-b)P_0, \quad (45b)$$

$$P_2 = 1/2 Q''(-1) = 1/2 [b + (a-b)^2] P_0, \quad (45c)$$

$$P_N = P_0 \sum_{k=0}^{\lfloor (N-1)/2 \rfloor} \frac{b^k (a-b)^{N-2k}}{2^k k! (N-2k)!}, \quad (45d)$$

where $[n]$ is the integer part of n , $[n - 1/2] \equiv n$.

Measurement of the distribution of the number of flashes makes it possible to determine with the aid of (45) the quantum efficiency of an image converter. Let $N^{(0)} + \eta N^{(1)} \ll 2\eta N^{(2)}$, then $b = \eta a$ and if $a \ll 1$ then $\eta = P_2/P_1$ (the background flashes can be excluded by additional measurements). In the second method one measures $\langle N \rangle$ and $\langle N^2 \rangle$. According to (45a) we have

$$\eta = (\langle N^2 \rangle - \langle N \rangle^2) / \langle N \rangle - 1.$$

We consider now the possibility of observing the influence of the statistics of the field on the photoprocess. The paired grouping of grains in emulsion under the action of TPL is apparently not easy to observe, owing to the multi-photon character of the photoprocess—for a exposure center to be produced, the silver-bromide microcrystal must absorb not less than two photons.¹¹

Two-photon light can influence, besides on the grain statistics, also the form of the density curve $D(I_0)$, where D is the optical density of the negative without allowance for fog. We assume for simplicity that the photoprocess is two-photon, and then at small exposures D is equal to the probability

of absorbing two photons in the microcrystal:

$$D = 1/2 (\sigma T \bar{I}^{(2)})^2 = 1/2 \sigma^2 H (H + 1/\bar{A}_{\text{eff}}^{(2)}), \quad (46)$$

where $\sigma \equiv \eta A$ and η are the cross sections probabilities of absorbing one photon in the microcrystal (we assumed that $A \ll \bar{A}^{(2)}$ and $T \gg t^{(2)}$, so that Eqs. (34)–(37) are valid). Thus, in the case of TPL the density curve $D(I_0)$ acquires a linear section at $H \ll 1/\bar{A}_{\text{eff}}^{(2)} = \pi/2\lambda_1 l$. Observation of this section would make possible absolute measurements of H (in units of $1/\bar{A}_{\text{eff}}^{(2)}$) and σ (in units of $\bar{A}_{\text{eff}}^{(2)}$). However, the threshold exposure (in photons per unit area) $1/\bar{A}_{\text{eff}}^{(2)}$, which separates the linear and quadratic sections, is quite small and in principle cannot exceed λ^{-2} corresponding to an energy density \hbar with $\lambda^{-3} \sim 10^{-9} \text{ J/cm}^2$.

CONCLUSION

A random transverse grouping of photons in random light at $\langle n \rangle \ll 1$ is used to measure the diameters of stars¹², and at $\langle n \rangle \gg 1$ it manifests itself in the form of "speckles." The paired grouping described here can be of interest for absolute quantum photometry, as well as from a heuristic point of view.

Observation of two-photon transitions under the influence of TPL, when using adjustable shift and delay between the photons in the pairs can apparently yield information on the dynamics of the transitions.

The results of the presented analysis agree quantitatively with the illustrative representation of photons as wave packets of size $\rho^{(1)}$ and $ct^{(1)}$. The biphotons are represented here in the form of two packets separated by distances $\rho^{(2)}$ and $ct^{(2)}$ in the transverse and longitudinal directions. Near the creation point and in the region of its imaging by the lens, the packets overlap, and this increases of the amplitude of the field and of its two-photon efficiency. On the image-converter cathode the packets are reduced into points of photoelectron emission.

We note that paired transverse grouping of photons should manifest itself also in four-photon parametric scattering, in incoherent parametric scattering by individual molecules,¹⁰ and in spontaneous two-photon decay, direct or cascaded.

We note, finally, the possibility of transverse antigrouping—the points have on the screen a distribution more uniform than the Poisson distribution.

The author thanks V. B. Braginskii for interest in the work and for stimulating discussions.

¹B. Ya. Zel'dovich and D. N. Klyshko, Pis'ma Zh. Eksp. Teor. Fiz. **9**, 69 (1969) [JETP Lett. **9**, 40 (1969)].

²D. C. Burnham and D. L. Weinberg, Phys. Rev. Lett. **25**, 84 (1970).

³D. N. Klyshko, Kvant. Elektron. (Moscow) **4**, 1056 (1977); **7**, 1932 (1980) [Sov. J. Quantum Electron. **7**, 755 (1977); **10**, 1112 (1980)].

⁴A. A. Malygin, A. N. Penin, and A. V. Sergienko, Pis'ma Zh. Eksp. Teor. Fiz. **33**, 493 (1981) [JETP Lett. **33**, 477 (1981)].

⁵K. J. McNeil and D. F. Walls, Phys. Lett. **51** A, 233 (1975).

⁶I. V. Sokolov, Zh. Eksp. Teor. Fiz. **72**, 1687 (1977) [Sov. Phys. JETP **45**, 884 (1977)].

⁷V. M. Petnikova, Kvant. Elektron. (Moscow) **6**, 456 (1979) [Sov. J. Quantum Electron. **9**, 276 (1979)].

⁸R. J. Glauber, Phys. Rev. **131**, 2766 (1963).

⁹E. Granneman and M. Van der Viel, J. Phys. **B8**, 1617 (1975).
¹⁰N. B. Baranova and B. Ya. Zel'dovich, Zh. Eksp. Teor. Fiz. **71**, 727
(1976) [Sov. Phys. JETP **44**, 383 (1976)].
¹¹T. H. James, Theory of the Photographic Process [Russ. Transl.], Khi-

miya, 1980.
¹²R. Hanbury-Brown, Contemp. Phys. **12**, 357 (1971).

Translated by J. G. Adashko